

Akinori Hasegawa,<sup>a,\*</sup> Yoshiteru Itagaki<sup>b</sup> and Masaru Shiotani<sup>b</sup>

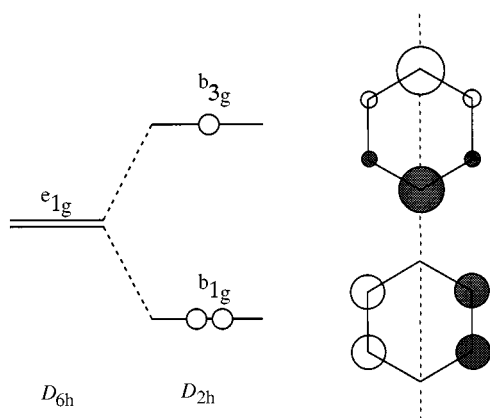
<sup>a</sup> Department of Chemistry, Kogakkan University, Ise-shi 516, Japan

<sup>b</sup> Department of Applied Chemistry, Faculty of Engineering, Hiroshima University, Higashi-Hiroshima 739, Japan

EPR spectra for the radical cations of a series of fluorinated benzenes, generated by irradiation with  $\gamma$ -rays in halocarbon solid matrices, have been observed at low temperatures. The spectra consist of a hyperfine structure with axially symmetric anisotropy mainly due to fluorine nuclei. The observed spectra have been analysed by simulation. *Ab initio* calculations have been conducted for the cation radicals to obtain their optimized geometries. The results reveal that an unambiguous deformation in geometry is brought about by cationization in each case. INDO calculations have been performed for the optimized geometries of these radical cations to calculate the hyperfine couplings. The calculated couplings strongly support the observed ones. The symmetry of the SOMO for the radical cations resembles that of the HOMO of their neutral mother molecules. The deformed geometries of these radical cations suggests that in the process of releasing an electron from an HOMO, those chemical bonds with bonding nature in the HOMO become elongated and those bonds with antibonding nature become shortened. It is concluded that the structure and symmetry of the SOMO of these radical cations are affected not only by the number of substitutions by fluorine but also by the position of substitution.

## Introduction

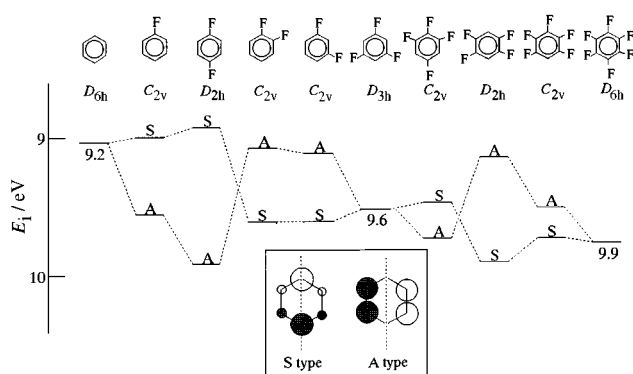
Radical cations of benzene formed in Freon ( $\text{CCl}_3\text{F}$ ) matrices at 4 K have been investigated by means of the EPR method.<sup>1</sup> The EPR spectra of the cations observed at the same temperature suggest that the orbital degeneracy of  $e_{1g}(D_{6h})$  for neutral benzene is removed by a static Jahn–Teller effect upon release of one electron and that the unpaired electron occupies a  $b_{3g}(D_{2h})$  SOMO<sup>2,3</sup> giving major hyperfine couplings to two H nuclei, as shown in Scheme 1. However, at elevated temp-



**Scheme 1** Schematic representation for the electronic state of the benzene cation. When the  $D_{6h}$  benzene ring is distorted to a  $D_{2h}$  structure by a static Jahn–Teller effect in the process of cationization, the highest occupied  $e_{1g}$  orbitals, doubly degenerated, split into  $b_{1g}$  and  $b_{3g}$  orbitals. Thus, the SOMO is either the  $b_{1g}$  orbital for the cation in an elongated  $D_{2h}$  geometry or the  $b_{3g}$  orbital for the cation in a compressed  $D_{2h}$  geometry.<sup>3</sup> The  $b_{3g}$  SOMO has been strongly supported by the observed EPR spectra with large couplings to two H nuclei.<sup>1</sup> The  $z$  axis is along the major  $C_2$  symmetry axis (dashed line) and the  $y$  axis is perpendicular to the ring plane.

eratures (higher than *ca.* 100 K) dynamic averaging arises resulting in a hyperfine structure (hfs) due to six equivalent H nuclei.

As regards the ionic radicals of fluorinated aromatic derivatives, a number of spectroscopic and theoretical studies have been carried out and their molecular and electronic structures have been discussed with reference to the substituent effect of fluorine.<sup>4</sup> The ionization potentials (IPs) of these derivatives obtained by photoelectron spectroscopy gave information on the energy levels. IPs become higher and the stability of the molecules increases with an increase in the number of fluorines substituted for the hydrogens of benzene,<sup>5,6</sup> as shown in Scheme 2. Together with the CNDO/S2 MO calculation results, they



**Scheme 2** Energy levels showing the first two ionization potentials from PE spectra with the symmetry of MOs for a series of fluorinated benzenes.<sup>5,6</sup> The symmetry of MOs of S or A type depends on whether they are symmetric or antisymmetric under reflection in the plane passing through the  $C_1$  and  $C_4$  carbons, perpendicular to the ring. See Fig. 5 for the  $C_1$  and  $C_4$  carbons of *o*- and *m*- $\text{C}_6\text{H}_4\text{F}_2$ .

were discussed in terms of the ‘perfluoro effect’<sup>7</sup> resulting from an ‘inductive (stabilization) effect’ for the  $\sigma$  bonds of the fluorine atoms and a ‘plus inductive (destabilization) effect’ for the  $\pi$  electrons of the atoms.<sup>6</sup>

On the other hand, EPR can provide information on spin density distribution and suggest the symmetry of the SOMO which reflects the HOMO and the LUMO of the mother

molecules in the case of radical cations and anions, respectively, if the structure of the ionic radicals is similar to that of the mother molecules. These MOs are useful in providing information on, for example, the reactivity of the molecules as the Frontier Electron Theory teaches us.<sup>8</sup>

The EPR spectra of  $C_6F_6^+$  generated in a  $c-C_6F_{12}$  matrix have been recently investigated by the present authors,<sup>9</sup> together with those of the  $C_6F_6^-$  anion. The  $C_6F_6^+$  spectrum at low temperatures consists of an axially symmetric triple quintet with  $A_{\parallel} = 1.35$  mT and  $A_{\perp} = 9.85$  mT due to equivalent two and four  $^{19}F$  nuclei, respectively, and they were successfully interpreted in terms of a  $D_{2h}$  structure in a  ${}^2B_{2g}$  state with an elongated ring, although, in addition to the  ${}^2B_{2g}$  state, a  ${}^2B_{3g}$  state with a compressed ring was also suggested from MO calculations.<sup>10</sup> The  $D_{2h}$  structure has three  $C_2$  symmetry axes, and the  $z$  axis was chosen to coincide with the axis perpendicular to the ring in the studies on the  $C_6H_6^+$  and  $C_6F_6^+$  cations.<sup>3,9</sup> However, when the cations of a series of fluorobenzenes are investigated, it is better to take the  $z$  axis along the major  $C_2$  axis in the ring plane and to take the  $y$  axis perpendicular to the ring. For this choice,  $B_{3g}(b_{3g})$  is unchanged, but  $B_{2g}(b_{2g})$  is changed to  $B_{1g}(b_{1g})$ . This axial system is thus used in this paper. It is of interest to note that  $C_6H_6^+$  has a compressed  $D_{2h}$  structure with an unpaired electron in the  $b_{3g}$  orbital, while  $C_6F_6^+$  has an elongated  $D_{2h}$  structure with an electron in the  $b_{1g}$  orbital, in spite of the similar  $D_{6h}$  structures of the neutral molecules.

The radical cations of fluoro-substituted pyridines have been also studied by EPR spectroscopy.<sup>11</sup> The symmetry of the SOMO for the cations was obtained from an analysis of the hfs due to  $^{19}F$  nuclei with axially symmetric anisotropy.

A preliminary EPR study has been carried out for the radical cations of a series of fluoro-substituted benzenes,<sup>12</sup> but the details have not yet been reported. Therefore, in this study, full details of the study will be presented, together with the results of MO calculations for the radical cations by *ab initio* and semiempirical methods.

## Experimental

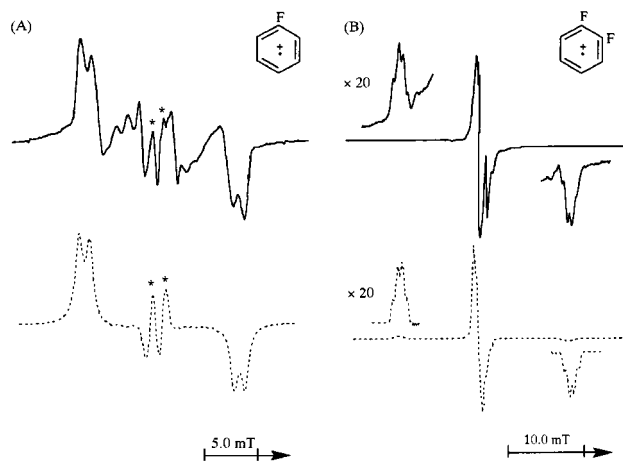
Commercially available reagents were used for a series of fluorinated benzenes. Solutions containing *ca.* 1 mol% of these fluorinated benzenes in either fluorotrichloromethane ( $CCl_3F$ ) or perfluorocyclohexane ( $c-C_6F_{12}$ ) were prepared in Spectrosil EPR sample tubes on a vacuum line. The samples were irradiated with  $\gamma$ -rays from a  ${}^{60}Co$  source at 77 K, the typical total absorption dose being *ca.* 1 Mrad. EPR measurements were carried out with a JEOL JES-PX-1X or Bruker ESP-300E X-band spectrometer operating at 100 kHz modulation and at variable temperatures using an Oxford continuous flow cryostat ESR 900. The field strength was measured using a Bruker EP 035M NMR Gaussmeter.

*Ab initio* calculations were carried out on a Cray J932/24 computer at the Information Processing Center, Hiroshima University, with 3-21 G basis sets, using the GAUSSIAN 94 program,<sup>13</sup> to obtain optimized geometries for the radical cations of the fluorinated benzenes. In order to calculate spin densities and hf couplings for atoms in the radical cations, INDO calculations<sup>14</sup> were performed for the geometries optimized by the *ab initio* method.

## Results and discussion

### EPR spectra and their assignments for the cations

The radical cations of a series of fluorinated benzenes were detected by the EPR method using either  $CCl_3F$  ( $IP_1 = 11.8$  eV)<sup>15</sup> or  $c-C_6F_{12}$  ( $IP_1 = 12.9$  eV)<sup>16</sup> as matrices at 77 K. The  $c-C_6F_{12}$  matrices are more effective for heavily fluorinated benzenes because their IPs increase with an increase in the number of substituted fluorines. The observed anisotropic EPR spectra show well-defined features for the parallel components



**Fig. 1** First derivative X-band EPR spectra for solid solutions of *ca.* 1 mol% of fluorobenzene (A) and *o*-difluorobenzene (B) in trichlorofluoromethane after irradiation at 77 K, observed at 93 K (A) and 77 K (B), and the lower spectra (dashed lines) are those simulated using the EPR parameters for the corresponding radical cations in Table 1. The signals marked \* in (A) correspond to the perpendicular components of the anisotropic hfs. In the observed spectrum, one of the signals is partly masked by signals from matrix radicals.

of axially symmetric hf coupling to  $^{19}F$  nuclei and are photo-bleached by visible light.

**The  $C_6H_5F^+$  cation.** The unambiguous parallel components of a doublet were observed in the outermost regions of the EPR spectrum of an irradiated solid solution of  $C_6H_5F$  in  $CCl_3F$  observed at 93 K, as shown in Fig. 1(A). The main doublet may be assigned to the  $^{19}F$  nucleus and the additional one to the  $^1H$  nucleus in the *para*-position of  $C_6H_5F$ . Thus the observed spectrum may suggest the formation of the radical cation of  $C_6H_5F$ .

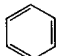

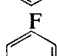
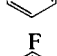
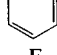
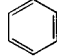
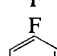
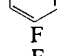
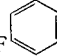
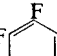
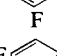
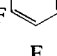
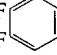
Spectral simulations were performed for an axially symmetric  $g$  tensor, an axially symmetric  $^{19}F$  hf tensor for the main doublet and an almost isotropic tensor for the additional doublet with a smaller coupling due to one  $^1H$ , using a second-order treatment. The spectrum simulated with the EPR parameters listed in Table 1 is shown in Fig. 1(A). The discrepancy between the observed and the simulated spectra may result mainly from the fact that the signals of some radicals probably formed from the  $CCl_3F$  matrix appear rather strongly in the central part of the observed spectrum for this system.

Similar EPR spectra were observed for an irradiated solid solution of  $C_6H_5F$  in  $c-C_6F_{12}$ . Hf coupling to  $^{19}F$  for the cation in the  $c-C_6F_{12}$  matrix is smaller than that in the  $CCl_3F$  matrix, as shown in Table 1.

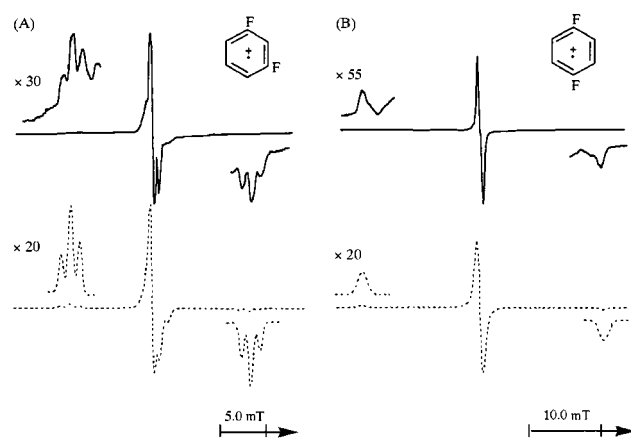
**The  $o-C_6H_4F_2^+$  cation.** The spectrum of an irradiated solid solution of  $o-C_6H_4F_2$  in a  $CCl_3F$  matrix showed parallel features with small additional splittings in the wing regions, as shown in Fig. 1(B). The main features were thought to be the outermost parallel components of a 1:2:1 triplet due to two equivalent  $^{19}F$  nuclei and the additional splittings to be a doublet. Judging from the symmetry of  $o-C_6H_4F_2$ , the additional triplet may originate from the two  $^1H$  nuclei in the 3,6- or 4,5-positions, but the doublet is difficult to assign to one  $^1H$  nucleus in the  $o-C_6H_4F_2$  molecule. The doublet may thus be assigned to the  $^{19}F$  nucleus of  $CCl_3F$ , as reported in the case of *e.g.*  $C_2F_4^+$ .<sup>17,18</sup> For the assignment of the two H nuclei, the theoretical calculations mentioned below may be helpful. Simulation with the parameters for  $o-C_6H_4F_2^+$  in Table 1 gave satisfactory results, see Fig. 1(B).

**The  $m-C_6H_4F_2^+$  cation.** Parallel features with a well-defined triplet were observed at the wings of the spectra of irradiated solid solutions of  $m-C_6H_4F_2$  in both  $CCl_3F$  [Fig. 2(A)] and  $c-C_6F_{12}$  matrices. The main features may be attributed to a triplet from two equivalent  $^{19}F$  nuclei and the additional triplet to the  $^1H$  nuclei in the 4,6-positions of the  $m-C_6H_4F_2$  cation.

**Table 1** EPR parameters for the radical cations of fluorinated benzenes

Radical cation	Matrix	<i>T</i> /K	<i>g</i>	<i>A</i> /mT			$\rho_{2p\pi}(^{19}\text{F})^c$	Assigned position of $^{19}\text{F}$ and $^1\text{H}$	Ref.
				<i>A</i> <sub>  </sub>	<i>A</i> <sub>⊥</sub> <sup>a</sup>	<i>a</i> <sup>a,b</sup>			
	CCl <sub>3</sub> F	77	2.0028 2.0027			(-) (-) (-)		6H H <sub>1,4</sub> H <sub>2,3,5,6</sub>	1
	CCl <sub>3</sub> F	93	<i>g</i> <sub>  </sub> = 2.0032 <i>g</i> <sub>⊥</sub> = 2.0060	15.0 1.0	1.0 1.2	5.7 1.1	0.087	F <sub>1</sub> H <sub>4</sub>	present work
	c-C <sub>6</sub> F <sub>12</sub>	77	<i>g</i> <sub>  </sub> = 2.0036 <i>g</i> <sub>⊥</sub> = 2.0051	12.0 1.0	1.0 1.2	4.7 1.1	0.068	F <sub>1</sub> H <sub>4</sub>	present work
	CCl <sub>3</sub> F	77	<i>g</i> <sub>  </sub> = 2.003 <i>g</i> <sub>⊥</sub> = 2.008	12.0 0.8	0.3 0.4	4.2 0.5	0.072	F <sub>1,2</sub> H <sub>4,5</sub>	present work
	CCl <sub>3</sub> F	77	<i>g</i> <sub>  </sub> = 2.002 <i>g</i> <sub>⊥</sub> = 2.006	9.6 1.0	ca. 0 ca. 0	3.7 0.3	0.055	F <sub>1,3</sub> H <sub>4,6</sub>	present work
	c-C <sub>6</sub> F <sub>12</sub>	77	<i>g</i> <sub>  </sub> = 2.002 <i>g</i> <sub>⊥</sub> = 2.006	9.3 1.0	0.7 ca. 0	3.6 0.3	0.053	F <sub>1,3</sub> H <sub>4,6</sub>	present work
	CCl <sub>3</sub> F	77	<i>g</i> <sub>  </sub> = 2.002 <i>g</i> <sub>⊥</sub> = 2.003	15.6 5.0	0.3 ca. 0	5.4 0.2	0.092	F <sub>1,4</sub> 4H	present work
	c-C <sub>6</sub> F <sub>12</sub>	84	<i>g</i> <sub>  </sub> = 2.002 <i>g</i> <sub>⊥</sub> = 2.006	15.0 12.7 6.4	0.7 0.7 0.7	5.5 4.7 2.6 0.6	0.088 0.074 0.035	F <sub>1</sub> F <sub>4</sub> F <sub>2</sub> H <sub>5</sub>	present work
	c-C <sub>6</sub> F <sub>12</sub>	140	<i>g</i> <sub>  </sub> = 2.003 <i>g</i> <sub>⊥</sub> = 2.004	4.94	ca. 0	1.7 0.7	0.029	F <sub>1,3,5</sub> H <sub>2,4,6</sub>	present work
	c-C <sub>6</sub> F <sub>12</sub>	77	<i>g</i> <sub>  </sub> = 2.002 <i>g</i> <sub>⊥</sub> = 2.006	16.9 12.7 2.8	0.3 0.3 0.3	5.8 4.4 1.1	0.101 0.076 0.018	F <sub>1</sub> F <sub>4</sub> F <sub>2,6</sub>	present work
	c-C <sub>6</sub> F <sub>12</sub>	77	<i>g</i> <sub>  </sub> = 2.002 <i>g</i> <sub>⊥</sub> = 2.006	10.9 0.5	ca. 0 ca. 0	3.8 0.2	0.064	2H F <sub>1,2,4,5</sub> 2H	present work
	c-C <sub>6</sub> F <sub>12</sub>	93	<i>g</i> <sub>  </sub> = 2.002 <i>g</i> <sub>⊥</sub> = 2.006	10.8 10.4	1.3 1.3	4.5 4.3	0.059 0.055	F <sub>2,6</sub> F <sub>3,5</sub>	present work
	c-C <sub>6</sub> F <sub>12</sub>	10	<i>g</i> <sub>  </sub> = 2.002 <i>g</i> <sub>⊥</sub> = 2.006	(-) 9.9	(-) 0.0	(-) 0.5 3.3	-0.006 -0.009 0.061	F <sub>1</sub> F <sub>1,4</sub> F <sub>2,3,5,6</sub>	9

<sup>a</sup> Error limit is  $\pm 0.3$  mT. <sup>b</sup> Isotropic hf splitting. <sup>c</sup> Spin density in  $2p_{\pi}(^{19}\text{F})$  orbital evaluated using the magnetic parameters listed by Goodman and Raynar.<sup>20</sup>



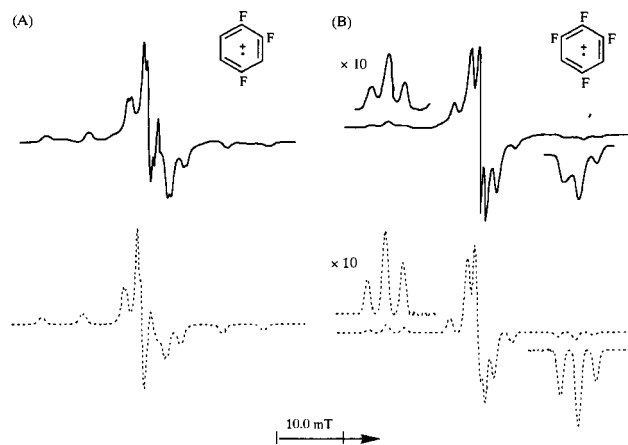
**Fig. 2** First derivative X-band EPR spectra for solid solutions of ca. 1 mol% of *m*-difluorobenzene (A) and *p*-difluorobenzene (B) in trichlorofluoromethane after irradiation at 77 K, observed at 77 K, and the lower spectra (dashed lines) are those simulated using the EPR parameters for the corresponding radical cations in Table 1

The spectrum simulated with the parameters for the cation in Table 1 may explain the observed spectrum, as can be seen in Fig. 2(A).

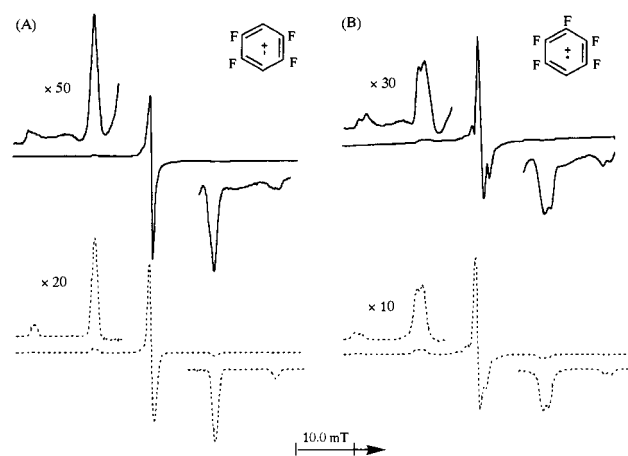
**The  $p\text{-C}_6\text{H}_4\text{F}_2^+$  cation.** Poorly resolved parallel features were observed in the spectrum of an irradiated solid solution of  $p\text{-C}_6\text{H}_4\text{F}_2$  in CCl<sub>3</sub>F, as shown in Fig. 2(B). The triplet may be due to two  $^{19}\text{F}$  nuclei. Judging from the molecular symmetry, the additional splittings may result from four equivalent  $^1\text{H}$  nuclei of the  $p\text{-C}_6\text{H}_4\text{F}_2^+$  cation. The coupling constant was estimated by simulation, as shown in Fig. 2(B).

**The 1,2,4- $\text{C}_6\text{H}_3\text{F}_3^+$  cation.** An EPR spectrum consisting of many well-defined lines was obtained for an irradiated solid solution of 1,2,4- $\text{C}_6\text{H}_3\text{F}_3$  in c-C<sub>6</sub>F<sub>12</sub>, as shown in Fig. 3(A). This spectrum was almost perfectly reproduced by the simulation performed using a *g*-tensor and hf tensors for three different doublets, the *g* and the hf tensors having the same principal direction, and an isotropic tensor for a doublet with a small coupling, as can be seen from Fig. 3(A). The former three doublets may be due to the  $^{19}\text{F}$  nuclei of 1,2,4- $\text{C}_6\text{H}_3\text{F}_3^+$  and the other doublet with the small coupling to a  $^1\text{H}$  of the cation. Theoretical calculations have to be waited for more detailed assignments.

**The 1,3,5- $\text{C}_6\text{H}_3\text{F}_3^+$  cation.** Only a broad signal was observed in the spectrum of an irradiated solid solution of 1,3,5- $\text{C}_6\text{H}_3\text{F}_3$  in c-C<sub>6</sub>F<sub>12</sub> measured at 77 K. The line-width was hardly reduced, even by cooling to 4 K, but did decrease on annealing. Measurement at 140 K gave a spectrum with poorly resolved features. This spectrum may be assigned to the 1,3,5- $\text{C}_6\text{H}_3\text{F}_3^+$



**Fig. 3** First derivative X-band EPR spectrum for solid solutions of *ca.* 1 mol% of 1,2,4-trifluorobenzene (A) and 1,2,4,6-tetrafluorobenzene (B) in perfluorocyclohexane after irradiation at 77 K, observed at 84 K (A) and 77 K (B), and the lower spectra (dashed lines) are those simulated using the EPR parameters for the corresponding radical cations in Table 1



**Fig. 4** First derivative X-band EPR spectrum for solid solutions of *ca.* 1 mol% of 2,3,5,6-tetrafluorobenzene (A) and pentafluorobenzene (B) in perfluorocyclohexane after irradiation at 77 K, observed at 77 K (A) and 93 K (B), and the lower spectra (dashed lines) are those simulated using the EPR parameters for the corresponding radical cations in Table 1

cation which has a structure distorted by the Jahn–Teller effect but is thermally averaged at this temperature, in a similar manner to  $C_6F_6^+$ . This spectrum was tentatively interpreted in terms of three equivalent  $^{19}F$  with a large coupling and three equivalent  $^1H$  with a small coupling, listed in Table 1.

**The 1,2,4,6- $C_6H_2F_4^+$  cation.** The spectrum of an irradiated solid solution of 1,2,4,6- $C_6H_2F_4$  in  $c-C_6F_{12}$  consists of parallel lines attributable to two doublets with different large couplings and a triplet with a smaller coupling, as shown in Fig. 3(B). The symmetry of the molecule suggests that the triplet results from the two equivalent  $^{19}F$  nuclei in the 2,6-positions. The assignment of the two different doublets may be suspended until theoretical calculations. This spectrum was satisfactorily reproduced by simulation with the parameters listed in Table 1, as shown in Fig. 3(B).

**The 2,3,5,6- $C_6H_2F_4^+$  cation.** An axially symmetric anisotropic spectrum of a quintet was observed for an irradiated solid solution of 2,3,5,6- $C_6H_2F_4$  in  $c-C_6F_{12}$ , as shown in Fig. 4(A). The quintet may be due to the four equivalent  $^{19}F$  nuclei of the 2,3,5,6- $C_6H_2F_4$  cation. This spectrum was perfectly reproduced by simulation for the parameters in Table 1, as can be seen in Fig. 4(A).

**The  $C_6HF_5^+$  cation.** The spectrum observed for an irradiated solid solution of  $C_6HF_5$  in  $c-C_6F_{12}$  seems to be attributable to

a double quintet. However, simulation has revealed that instead of a quintet, two triplets with slightly different couplings listed in Table 1 gave a more satisfactory result, as shown in Fig. 4(B). The doublet with a small coupling may be assigned to the central  $^{19}F$  in the 1-position (*para*-position with respect to H). Assignment of the two different triplets must also be suspended.

**The  $C_6F_6^+$  cations.** The authors have already reported on the EPR spectra and structure of the radical cation,  $C_6F_6^+$ , in connection with those of the radical anion,  $C_6F_6^-$ .<sup>9</sup> Thus, a summary of the results for  $C_6F_6^+$  is given here in order to enable us to compare it with the radical cations under investigation.

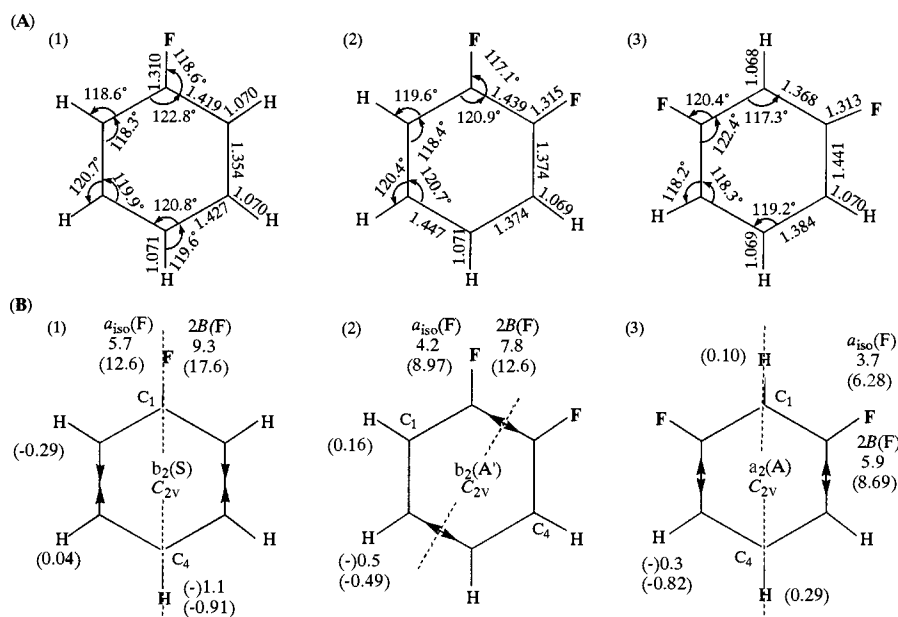
The EPR spectra of the  $C_6F_6^+$  cation generated in a solid solution of  $c-C_6F_{12}$  at 77 K dramatically depended upon the temperature of observation. The 170 K spectrum clearly showed seven equally spaced hyperfine lines due to six equivalent F nuclei, giving the EPR parameters of  $A_{||} = 6.77$  mT and  $A_{\perp} = ca. 0$  mT for the six nuclei and  $g_{||} = 2.0020$  and  $g_{\perp} = 2.0060$ . With decreasing temperature, the inner hyperfine lines became broader but the outermost lines remained unchanged. With further decreasing temperature, the outermost bands became sharper and then they split into three lines with an equal splitting of 1.35 mT at 10 K. Thus, the six fluorines of  $C_6F_6^+$  can be divided into two groups: one is the two equivalent fluorines  $A_{||} 1.35$  mT, and the other is four equivalent fluorines  $A_{||} 9.85$  mT.

The parent  $C_6F_6$  molecule has doubly degenerate HOMOs, but the orbital degeneracy is removed in the process of cationization. The symmetry of the SOMO of the radical cation can be determined by the HOMO from which one electron is released. *Ab initio* calculations for the cation suggested that two distorted  $D_{2h}$  structures are possible: an elongated ring structure with a  $b_{1g}$  SOMO and a compressed ring structure with a  $b_{3g}$  SOMO.<sup>3,10</sup> From the character of the SOMOs, a large splitting due to two equivalent F nuclei can be expected from the compressed structure, while a small splitting can be expected from the elongated one. The observed wing features of the triplet with a coupling of 1.35 mT may strongly suggest that the cation has a  $b_{1g}$  SOMO and an elongated  $D_{2h}$  structure.

It may be of interest to note that  $C_6F_6^+$  takes the elongated  $D_{2h}$  structure with the  $b_{1g}$  SOMO, whereas  $C_6H_6^+$  takes the compressed  $D_{2h}$  structure with the  $b_{3g}$  SOMO. *Ab initio* calculations gave two results.<sup>3</sup> At the UHF level, the elongated structure is 2.0 kcal mol<sup>-1</sup> more stable than the compressed structure for both  $C_6H_6^+$  and  $C_6F_6^+$ . On the other hand, at the level including electron correlation for the  $\pi$  electrons by means of second-order Møller-Plesset perturbation,<sup>19</sup> the compressed structure for  $C_6H_6^+$  and the elongated structure for  $C_6F_6^+$  are more stable, although the two distorted structures are within 0.1 kcal mol<sup>-1</sup> of each other in both cases.<sup>3</sup>

#### Spin densities in the radical cations

The anisotropic hyperfine couplings to  $^{19}F$  nuclei listed in Table 1 gave all of the radical cations studied a relation of  $A_{||}(^{19}F) \gg A_{\perp}(^{19}F) \cong 0$ , which is typical of  $\pi$ -radicals.<sup>17</sup> The spin densities in the  $2p_{\pi}$  orbitals of the  $^{19}F$  atoms can be obtained from the experimental anisotropic hyperfine couplings of  $A_{||}$  and  $A_{\perp}$  and the theoretical anisotropy in the hyperfine coupling of a  $^{19}F$  nucleus,  $2B^0 = 108.5$  mT.<sup>20</sup> Experimental  $A_{||}$  values were determined rather accurately from observed spectra, whereas  $A_{\perp}$  values were estimated approximately by simulation. In addition, the sign of the values for  $A_{\perp}$  is not known since the cases of both positive and negative signs were reported for the values of  $^{19}F$  in the  $\alpha$ -positions.<sup>21</sup> Therefore, both the cases were taken into account but positive signs were tentatively adopted for the calculation of spin densities for the radical cations. The spin densities thus obtained are also given in Table 1. Moreover, the fact that the principal directions of the  $^{19}F$  couplings coincide with one another in a molecule may also suggest planarity in the structure of the radical cations.



**Fig. 5** (A) Optimized geometrical structures for the radical cations of (1)  $C_6H_5F$ , (2)  $o-C_6H_4F_2$  and (3)  $m-C_6H_4F_2$  calculated with the GAUSSIAN 94 program at the UHF/3-21G level. The bond lengths are given in Å. (B) The experimental isotropic ( $a_{iso}$ ) and anisotropic ( $2B$ ) hf coupling constants to  $^1H$  and  $^{19}F$  nuclei (in mT) are compared with the theoretical ones (in parentheses) evaluated by the INDO MO method for the optimized structures. The arrows ( $\longleftrightarrow$ ) and ( $\rightarrow\leftarrow$ ) stand for the elongated and compressed, respectively, C-C bonds parallel to the axes passing through the  $C_1$  and  $C_4$  atoms. Major  $C_2$  symmetry axes are shown with dashed lines. Note that for the irreducible representation of the SOMO, an axial system was chosen to have the  $z$  axis along the major  $C_2$  symmetric axis and the  $y$  axis perpendicular to the ring, but that for S and A types, reflection was used in the plane passing through the  $C_1$  and  $C_4$  carbons, perpendicular to the ring. A' stands for A-like symmetry.

### Spin densities and hf coupling constants calculated by INDO

The EPR data will be discussed at a semiempirical level because high quality MO calculations on such high symmetry open-shell systems as these radical cations sometimes lead to pitfalls.<sup>22</sup> In advance of the semiempirical INDO calculations, however, the optimized geometries of these fluorinated benzene cations were obtained by *ab initio* calculations. Although we have to refrain from quantitative discussion of the results, we may be allowed to qualitatively speculate that a remarkable deformation was brought about by cationization in each case, as shown in Figs. 5(A)–7(A). As for the 1,3,5- $C_6H_3F_3^+$  cation, the geometry has not yet been optimized, probably because the cation is distorted by the Jahn-Teller effect. This radical cation will therefore be excluded in the following discussion.

INDO calculations were carried out for the geometries optimized by the *ab initio* method. Isotropic hf couplings to  $^1H$  and  $^{19}F$  were acquired from the  $s$ -spin densities on their nuclei obtained by INDO calculations and the atomic hf constants  $a_{iso}^0$  adjusted for INDO calculations, 53.986 and 4482.920 mT, respectively.<sup>14</sup> Anisotropic hf couplings,  $2B$ , to  $^{19}F$  nuclei were obtained from the  $p$ -spin densities on the nuclei and the atomic value calculated,  $2B^0 = 108.6$  mT.<sup>20</sup> These calculated values are shown with the observed values in Figs. 5(B)–7(B).

A comparison between the observed and calculated values strongly supported the assignments, directly made from the observed EPR spectra, not only to  $^{19}F$  of  $C_6H_5F^+$ ,  $C_6H_4F_2^+$  and 2,3,5,6- $C_6H_2F_4^+$  but also to  $^1H$  in the *para*-position of  $C_6H_5F^+$ ,  $^1H$  in the 4,6-positions of 1,3- $C_6H_4F_2^+$ ,  $^{19}F$  in the 2,6-positions of 1,2,4,6- $C_6H_2F_4^+$  and  $^{19}F$  in the 1-position (*para*-position with respect to H) of  $C_6HF_5^+$ . Moreover, as for the assignment of the 1:2:1 triplet to  $^1H$  of the 3,6- or 4,5-positions of  $o-C_6H_4F_2^+$ , it was concluded that the 4,5-positions were more reasonable. The four different doublets observed for 1,2,4- $C_6H_3F_3^+$ , which could not be identified from the EPR spectrum alone, were assigned to each of the  $^{19}F$  nuclei in the 1,2,4-positions and to  $^1H$  in the 5-position. Also, couplings to  $^{19}F$  in the 1,4-position in 1,2,4,6- $C_6H_2F_4^+$  and in the 2,6- and 3,5-positions of  $C_6HF_5^+$  were finally identified with the help of the

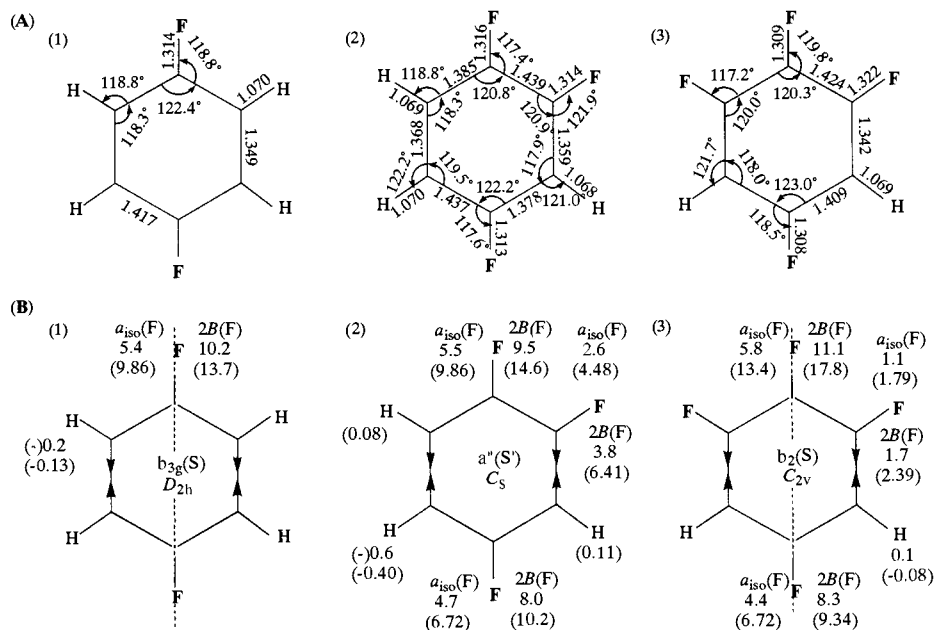
calculated results. The observed and assigned coupling constants are shown in Table 1 and the observed and calculated values for isotropic and anisotropic couplings are shown in Figs. 5(B)–7(B).

For these cations, the observed isotropic  $a_{iso}(^{19}F)$  and anisotropic  $2B(^{19}F)$  couplings are smaller than those calculated. However, good correlations were obtained between the observed  $a_{iso}(^{19}F)$  and calculated  $s$ -spin density on  $^{19}F$  and between the observed  $2B(^{19}F)$  and the calculated  $p$ -spin density on  $^{19}F$ , as shown in Fig. 8. The observed couplings ( $Y$ ) were related to the calculated spin densities ( $X$ ) by the linear function  $Y = CX$ , in both cases of  $a_{iso}(^{19}F)$  and  $2B(^{19}F)$ , the constant  $C$  being  $23.8 \times 10^2$  and 72.3 mT for  $a_{iso}(^{19}F)$  and  $2B(^{19}F)$ , respectively. The former is about one half of the atomic coupling of 4482.920 mT adjusted using only nine data for INDO calculations<sup>14</sup> and the latter is rather smaller than the calculated  $2B^0$  value of 108.6 mT.<sup>20</sup> This  $2B^0$  value has not been authorized for INDO calculations, but 50 mT was used as a parameter in the simulation of the EPR spectra of the  $C_6F_6$  anion radical.<sup>9</sup> In addition, one may remark that the values of  $A_{\perp}$  are not directly determined from the EPR spectra but are estimated by simulation and that the signs were not determined but were recorded as positive. When these  $C$  constants obtained were used, the calculated isotropic and anisotropic hf couplings coincide with the observed ones with very high correlation coefficients  $R$  of 0.94 and 0.95, respectively.

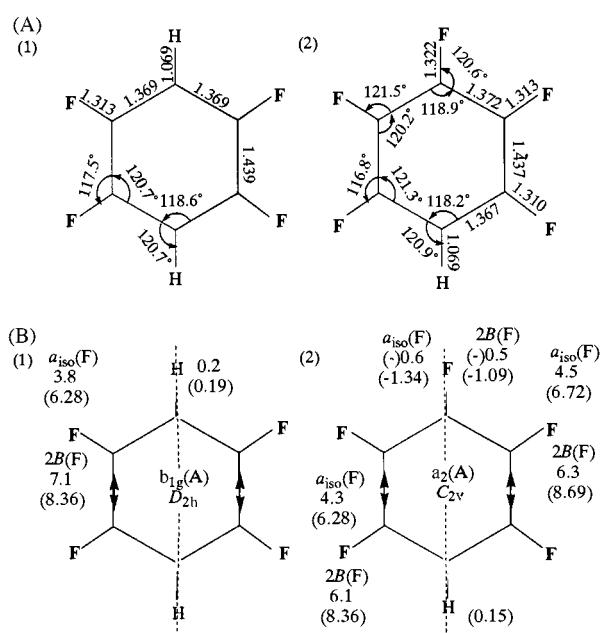
### The structure of the radical cations

Structural information on the radical cations investigated is already shown in the hf coupling data in Figs. 5(B)–7(B). This consists of the symmetry label of the irreducible representation of the SOMO, the type of SOMO labelled S or A in parentheses, the molecular point group and the arrows standing for the bonds elongated or compressed.

These results may not have quantitative meaning, but they may lead us to the following qualitative understanding. The symmetry of the SOMO in each radical cation resembles that of the HOMO in the corresponding neutral molecule. All of the deformed geometries of these radical cations under investig-



**Fig. 6** (A) Optimized geometrical structures for the radical cations of (1)  $p\text{-C}_6\text{H}_4\text{F}_2$ , (2)  $1,2,4\text{-C}_6\text{H}_3\text{F}_3$  and (3)  $1,2,4,6\text{-C}_6\text{H}_2\text{F}_4$  calculated with the GAUSSIAN 94 program at the UHF/3-21G level. The other caption for this figure can be seen in Fig. 5.  $S'$  stands for  $S$ -like symmetry.

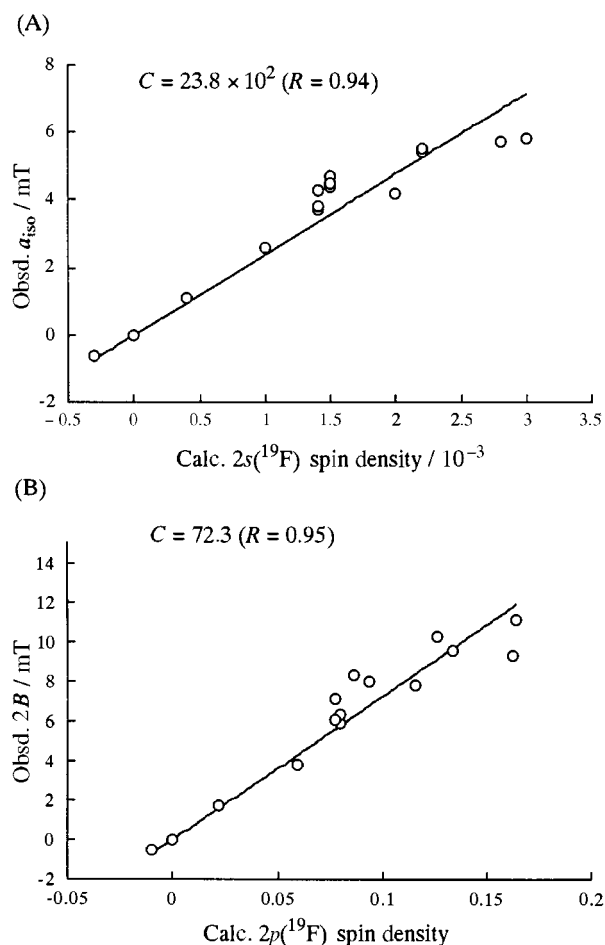


**Fig. 7** (A) Optimized geometrical structures for the radical cations of (1)  $2,3,5,6\text{-C}_6\text{H}_2\text{F}_4$  and (2)  $\text{C}_6\text{HF}_5$  calculated with the GAUSSIAN 94 program at the UHF/3-21G level. The other caption for this figure can be seen in Fig. 5.

ation imply that in the process of releasing one electron from an HOMO, the chemical bonds giving the bonding nature in the HOMO become elongated and the bonds giving the antibonding nature become shortened. The symmetry of the SOMOs of the radical cations is affected not only by the number of substitutions by fluorine but also by the position of substitution, and whether symmetry is of type  $S$  or type  $A$  is determined by the balance between the number of fluorines in the 1,4- and the 2,3,5,6-positions.

### Acknowledgements

The authors thank Messrs. H. Kawazoe and H. Toshiro for their assistance in the preliminary stage of this study. The present research was partially supported by the JSPS Program



**Fig. 8** The correlation between the observed hf coupling constants to  $^{19}\text{F}$  nuclei and the spin densities calculated by the INDO method for the *ab initio* optimized geometries. (A) and (B) are the plots for isotropic hf ( $a_{\text{iso}}$ ) vs.  $2s$  spin densities and for anisotropic hf ( $2B$ ) vs.  $2p$  spin densities, respectively. Constants ( $C$ ), i.e. the slopes of the fitted lines, and correlation coefficients ( $R$ ), are given in the Figure.

for supporting University-Industry Cooperative Research Project and the Subsidy for Scientific Research of the Ministry of Education in Japan (Grant No. 08240105).

## References

- 1 M. Iwasaki, K. Toriyama and K. Nunome, *J. Chem. Soc., Chem. Commun.*, 1983, 320.
- 2 The notation of  $b_{2g}(D_{2h})$  was used in ref. 1. However, the axial system described in the caption of Scheme 1 and used in this paper gives  $b_{3g}(D_{2h})$ . Also, see the text.
- 3 K. Raghavachari, R. C. Haddon, T. A. Miller and V. E. Bondybey, *J. Chem. Phys.*, 1983, **79**, 1387.
- 4 K. S. Chen, P. J. Krusic, P. Meakin and J. K. Kochi, *J. Phys. Chem.*, 1974, **78**, 2014; P. J. Krusic, K. S. Chen, P. Meakin and J. K. Kochi, *J. Phys. Chem.*, 1974, **78**, 2036; P. J. Krusic and P. Meakin, *J. Am. Chem. Soc.*, 1976, **98**, 228; J. T. Wang and F. Williams, *Chem. Phys. Lett.*, 1980, **71**, 471; Y. N. Molin and B. A. Anisimov, *Rad. Phys. Chem.*, 1983, **21**, 77; M. B. Yim and D. E. Wood, *J. Am. Chem. Soc.*, 1976, **98**, 2053; M. B. Yim, S. DiGregorio and D. E. Wood, *J. Am. Chem. Soc.*, 1977, **99**, 4260; C. R. Brundle, M. B. Robin, N. A. Kuebler and H. Basch, *J. Am. Chem. Soc.*, 1972, **94**, 1451; C. R. Brundle, M. B. Robin and N. A. Kuebler, *J. Am. Chem. Soc.*, 1972, **94**, 1466.
- 5 I. D. Clark and D. C. Frost, *J. Am. Chem. Soc.*, 1967, **89**, 244; J. R. Frazier, L. G. Carter and H. C. Schweinler, *J. Chem. Phys.*, 1978, **69**, 3807; J. A. Sell and A. Kupperman, *Chem. Phys.*, 1978, **33**, 367; K. D. Jordan and P. D. Burrow, *J. Chem. Phys.*, 1979, **71**, 5384; L. G. Christophorou and H. C. Schweinler, *J. Chem. Phys.*, 1979, **71**, 5385.
- 6 C. B. Duke, K. L. Yip, G. P. Ceasar, A. W. Potts and D. G. Streets, *J. Chem. Phys.*, 1977, **66**, 256.
- 7 See, for example: J. W. Rabalais, *Principles of Ultraviolet Photoelectron Spectroscopy*, Wiley, New York, 1977; D. W. Turner, C. Baker, A. D. Baker, and C. R. Brundle, *Molecular Photoelectron Spectroscopy*, Wiley, New York, 1970; C. R. Brundle, M. B. Tobin and N. A. Kuebler, *J. Am. Chem. Soc.*, 1972, **94**, 1466.
- 8 K. Fukui, T. Yonezawa and H. Shingu, *J. Chem. Phys.*, 1952, **20**, 722.
- 9 A. Hasegawa, M. Shiotani and Y. Hama, *J. Phys. Chem.*, 1994, **98**, 1834.
- 10 K. Hiraoka, S. Mizuse and S. Yamabe, *J. Phys. Chem.*, 1990, **94**, 3689.
- 11 M. Shiotani, H. Kawazoe and J. Shoma, *J. Phys. Chem.*, 1984, **88**, 2220.
- 12 M. Shiotani, H. Kawazoe and J. Shoma (a) *Proceedings of the 7th International Congress of Radiation Research*, A1-44, Martinus Nijhoff Publishers, Amsterdam, 1983; (b) *Proceedings of the 22nd Japanese ESR Symposium*, 1983, p. 127.
- 13 J. B. Foresman and AE. Frisch, *Exploring Chemistry with the Electronic Structure Method*, 2nd edn., Gaussian, Inc., Pittsburgh, PA, 1996.
- 14 J. A. Pople and D. L. Beveridge, *Approximate Molecular Orbital Theory*, McGraw-Hill, New York, 1970.
- 15 T. Shida, Y. Nosaka and T. Kato, *J. Phys. Chem.*, 1978, **82**, 695.
- 16 S. Katsumata and M. Shiotani, unpublished data.
- 17 A. Hasegawa and M. C. R. Symons, *J. Chem. Soc., Faraday Trans. 1*, 1983, **79**, 93.
- 18 G. W. Eastland, D. N. R. Rao, J. Rideout, M. C. R. Symons and A. Hasegawa, *J. Chem. Research (S)*, 1983, 258.
- 19 C. Møller and M. S. Plesset, *Phys. Rev.*, 1934, **46**, 618; J. S. Binkley and J. A. Pople, *Int. J. Quantum Chem.*, 1975, **9**, 229.
- 20 B. A. Goodman and J. B. Raynor, *Adv. Inorg. Chem. Radiochem.*, 1970, **13**, 135.
- 21 M. Iwasaki, S. Noda and K. Toriyama, *Molec. Phys.*, 1970, **18**, 201; M. Iwasaki, *Molec. Phys.*, 1971, **20**, 503.
- 22 The authors thank one of the referees for this comment.

Paper 7/03093B  
Received 6th May 1997  
Accepted 22nd May 1997